Metal–metal bonding in metal–string complexes $M_3(dpa)_4X_2$ (M = Ni, Co, dpa = di(2-pyridyl)amido, and X = Cl, NCS) from resonance Raman and infrared spectroscopy

Szu-Hsueh Lai [a], Chung-Jen Hsiao [a], Jung-Wei Ling [a], Wen-Zhen Wang [b], Shie-Ming Peng [b], I-Chia Chen [a],*

[a] *Department of Chemistry, National Tsing Hua University, 101 Kuang Fu Road Second Section, Hsinchu 30013, Taiwan, ROC*
[b] *Department of Chemistry, National Taiwan University, Taipei 10617, Taiwan, ROC*

ARTICLE INFO

ABSTRACT

Infrared and Raman spectra for metal–string complexes $M_3(dpa)_4X_2$ (M = Ni, Co, dpa = di(2-pyridyl)amido, and X = Cl, NCS) are studied. We assign the Ni_3 asymmetric stretching vibration to infrared lines at 304 and 311 cm^{-1} for $Ni_3(dpa)_2Cl_2$ and $Ni_3(dpa)_2(NCS)_2$, respectively. A Raman shift at 242 cm^{-1} is assigned to the Ni_3 symmetric stretching mode. For Co_3 complexes a line for the Co_3 asymmetric stretching mode appears at 313 and 331 cm^{-1} for $Co_3(dpa)_2Cl_2$ and $Co_3(dpa)_2(NCS)_2$, respectively.

1. Introduction

Metal complexes with polypyridyl ligands have attracted much attention because such a system has prospective applications as metal wires on a molecular scale [1–22]. According to structures determined with X-ray diffraction, these complexes have collinear metal ions and are coordinated with four ligands helically. The simplest complexes for these series have trimetal strings $M_3(dpa)_4X_2$ (dpa = di(2-pyridyl)amido). To understand the binding between metals, both a simple molecular-orbital model and quantum-chemical calculations with density-functional theory have been employed to interpret the bond strength and magnetic properties. According to a simple molecular-orbital model we expect no bonding between nickel ions in $Ni_3(dpa)_4X_2$ although the distance between two adjacent nickels is 2.42–2.44 Å, constrained by the ligand structure. Aduldecha and Hathaway [1] suggested the presence of two unpaired electron spins on the two terminal nickel metal ions and no unpaired electronic spin on the central Ni according to the measured magnetic moment 2.46 per Ni^{II} at room temperature. Clerac et al. [8] and Berry et al. [9] suggested an antiferromagnetic coupling of two terminal nickels through the central, diamagnetic Ni. For cobalt and chromium trimetal complexes, both symmetric and asymmetric metal–metal bonding structures are observed. The bond orders predicted for symmetric trimetal ions Co_3^{6+} and Cr_3^{6+} are 0.5–0.75 and 1.5, respectively [9,11,12]. The asymmetric structure consists of an isolated metal atom and a pair of metal atoms with direct metal–metal interaction, bond order = 1 and 4 for the tricobal and trichromium complexes, respectively. Scanning tunneling microscopy indicates that the conductance of

these metal–string complexes correlates well with the metal–metal bond order, with the conductance order $Cr_3^{6+} > Co_3^{6+} > Ni_3^{6+}$ for symmetric trimetal structures [19,20]. However the actual bonding strength between metals remains unclear.

Despite that there are plenty of examples for study of metal string complexes few literature reports concern spectra specifically for metal–metal bonding. Here we investigated the bonding strength of metal–metal bonds in complexes $M_3(dpa)_4X_2$ (dpa = di(2-pyridyl)amido; M = Ni, Co; X = Cl, NCS) using IR and Raman spectra. Their chemical structures and some relevant bond distances are displayed in Scheme 1. We include both structure isomers asymmetric and symmetric $Co_3(dpa)_4Cl_2$.

2. Experiments

The solid metal complexes and dipyridylamine, Hdpa were synthesized according to methods described elsewhere [1,2]. Compound $Co_3(dpa)_4Cl_2$ was purified by recrystallization from a CH_2Cl_2 solution at room temperature. IR absorption spectra in the far-infrared region 150–650 cm^{-1} were recorded at the NTHU Instrument Center (Bomem FTIR spectrometer). A solid sample was mixed with CsI at a ratio 1:1–2 for the low-frequency range to obtain sufficient absorbance. The Raman spectra were recorded in a backscattering geometry to improve the signal to noise ratio; the spectral resolution, 3 cm^{-1}, was limited by the monochromator (length 0.6 m, grating with 600 groove/mm). A He–Ne laser (wavelength 632.8 nm) served as the excitation source; the laser power at the sample was set at 15 mW. The scattered signal passing through a notch filter was recorded with a CCD detector. The integration period was typically about 30 s, and averaged for 100 scans. To avoid self-absorption for Raman measurements, a sample was mixed with KBr at a ratio 1:10. All spectra were recorded under room temperature.

---

* Corresponding author. Fax: +886 3 5721614.
E-mail address: icchen@mx.nthu.edu.tw (I-Chia Chen).
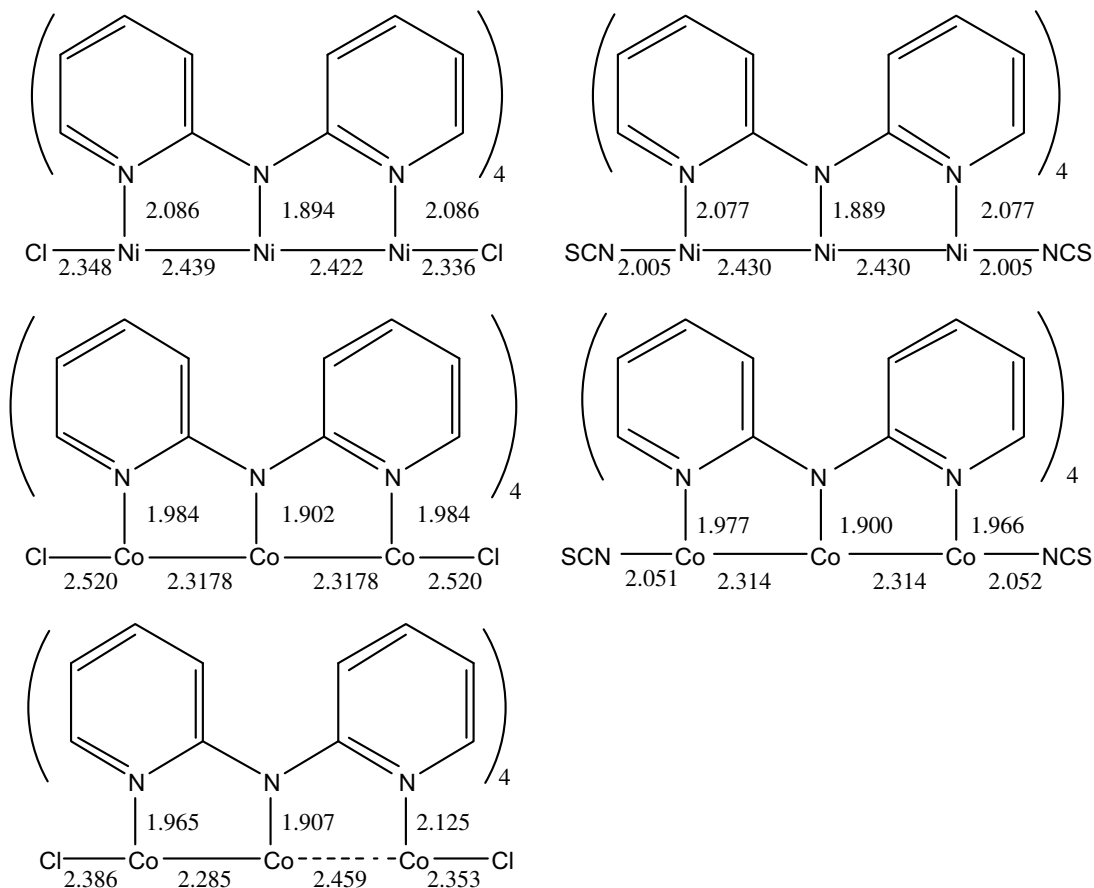
Scheme 1. Chemical structures of Ni$_3$(dpa)$_4$Cl$_2$, Ni$_3$(dpa)$_4$(NCS)$_2$, Co$_3$(dpa)$_4$(NCS)$_2$, and symmetric and asymmetric Co$_3$(dpa)$_4$Cl$_2$ and their bond distances/Å taken from Refs. [2,8,3,5], respectively.
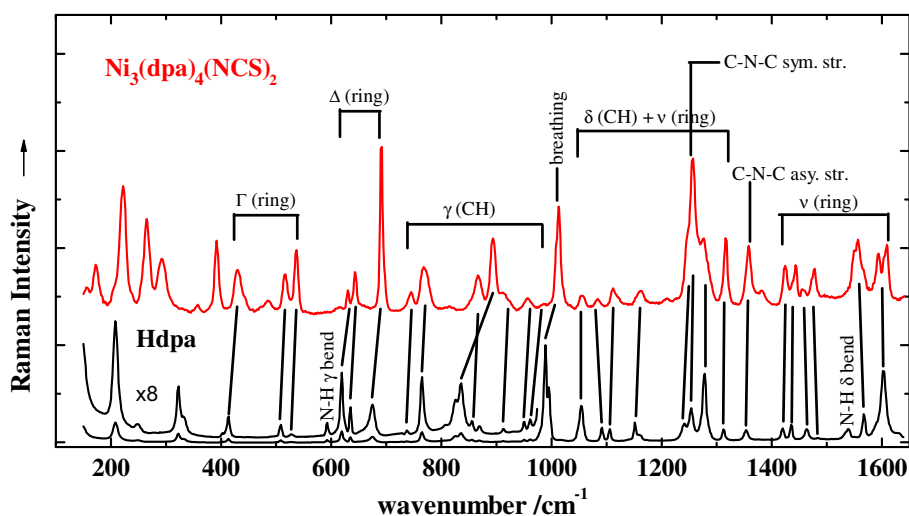
Fig. 1. Raman spectra (150–1650 cm^{-1}) of Ni$_3$(dpa)$_4$(NCS)$_2$ and Hdpa in the solid state, obtained with at excitation wavelength 632.8 nm. Symbol ν denotes a stretching mode, δ and γ for in-plane bending and out-of-plane bending of pyridyl and Γ and Δ for pyridyl–pyridyl ring–ring in-plane and out-of-plane twisting modes, respectively.

Quantum-chemical calculations based on density-functional theory (DFT) were performed to obtain optimized geometries, vibrational frequencies and both Raman and IR intensities for Hdpa. Method B3LYP at basis set 6-31 G* was employed to achieve reliable results. All calculations were performed with the GAUSSIAN 03 program [23].

3. Results and discussion

Raman spectra of Ni$_3$(dpa)$_4$(NCS)$_2$ and Hdpa in a region 150–1650 cm^{-1} are displayed in Fig. 1. The Raman and IR spectra of metal complexes exhibit features generally similar to those of Hdpa in the range 410–1600 cm^{-1}, in which most pyridyl vibrations are
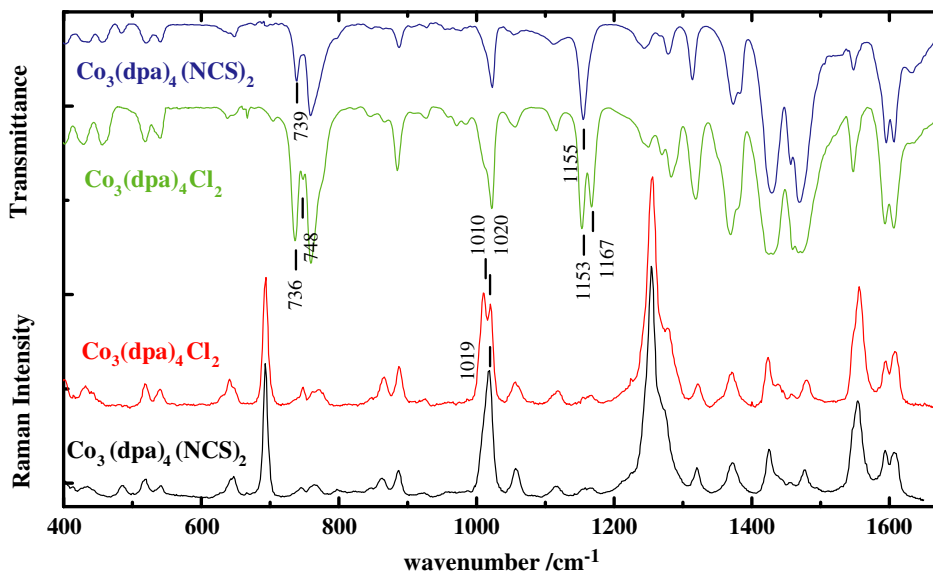
Fig. 2. IR and Raman spectra (400–1650 cm^{-1}) of Co$_3$(dpa)$_4$Cl$_2$ and Co$_3$(dpa)$_4$(NCS)$_2$.
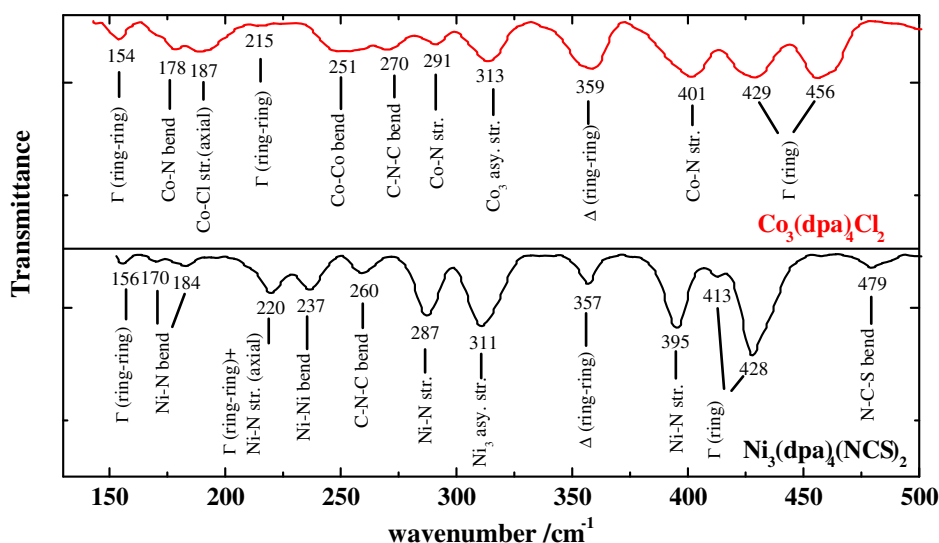
Fig. 3. IR spectra (150–500 cm^{-1}) of Ni$_3$(dpa)$_4$(NCS)$_2$ and Co$_3$(dpa)$_4$Cl$_2$ powder mixed with CsI (ratio 1:1). Symbols are defined in the caption of Fig. 1.

located. From the known assignments of vibrational normal modes for pyridyl and on comparison with spectra calculated using the DFT method, most Hdpa spectral lines are assignable. Because the calculated results are based on an isolated structure whereas Hdpa in a solid form has hydrogen bonding between two molecules, the experimental lines are broadened and might even split, for example in the region ~840 cm^{-1}. Lines for the N–H out-of-plane bending mode appearing at 595 cm^{-1} and in-plane bending mode at 1532 cm^{-1} for Hdpa disappear in metal complexes because of deprotonation upon formation. The C–N–C in-plane bending mode at 836 cm^{-1} for Hdpa becomes accordingly blue shifted to 894 cm^{-1} as that in Ni$_3$(dpa)$_4$Cl$_2$.

The pyridyl lines for Ni$_3$(dpa)$_4$(NCS)$_2$ at 741 (IR), 1013 (Raman) and 1154 (IR) cm^{-1} split to 736 and 748 cm^{-1}, 1010 and 1020 cm^{-1} and 1153 and 1167 cm^{-1}, respectively for Co$_3$(dpa)$_4$Cl$_2$ indicating existence of two distinct pyridyl groups, shown in Fig. 2. For Co$_3$(dpa)$_4$(NCS)$_2$ these lines remain single under our experimental conditions. Complex Co$_3$(dpa)$_4$Cl$_2$ has asymmetric and symmetric isomers, and for the asymmetric isomer with two distinct Co–Co bonding consequently producing two distinct pyridyls in an asym-

metric structure. In IR spectra for both solid samples, Clearc et al. [10] assigned the line at 1154 cm^{-1} (or 1153 cm^{-1}) to contribute from both structures; from the spectral intensities we estimate the symmetric and asymmetric structures in a chloride sample at ratio 1:4 approximately.

Metal–metal, metal–ligand, and ligand pyridyl–pyridyl, ring–ring out-of-plane vibrations have frequencies below 450 cm^{-1}. These modes are the most sensitive to reveal the strength of metal–metal bonding. Hence we show the spectra in the low-frequency region. Fig. 3 shows IR spectra of Ni$_3$(dpa)$_4$(NCS)$_2$ and Co$_3$(dpa)$_4$Cl$_2$, with IR and Raman spectra of Ni$_3$(dpa)$_4$Cl$_2$ for comparison in Fig. 4, and in Fig. 5 Raman spectra of Ni$_3$(dpa)$_4$(NCS)$_2$ and Co$_3$(dpa)$_4$Cl$_2$. We expect that pyridyl–pyridyl twisting modes should be the least variable on altering the metal or axial-ligand. Comparing spectra of all four complexes, we hence assign the pyridyl, pyridyl–pyridyl, ring–ring out-of-plane and C–N–C bending vibrations to be at 428, 356 and 265 cm^{-1}, respectively for Ni$_3$(dpa)$_4$Cl$_2$. Other complexes at similar positions are shown in Figs. 3–5.

We assign the metal–metal and metal–ligand vibrations according on the following basis. Many authors have reported the
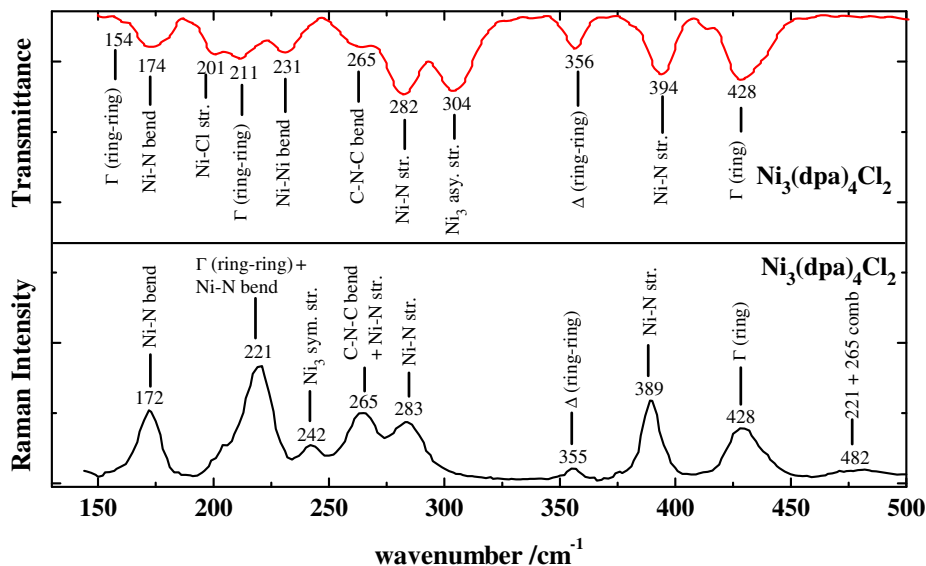
Fig. 4. IR (upper trace) and Raman (lower trace) spectra of $Ni_3(dpa)_4Cl_2$ in a region 150–500 cm^{-1}. Symbols are defined in the caption of Fig. 1.
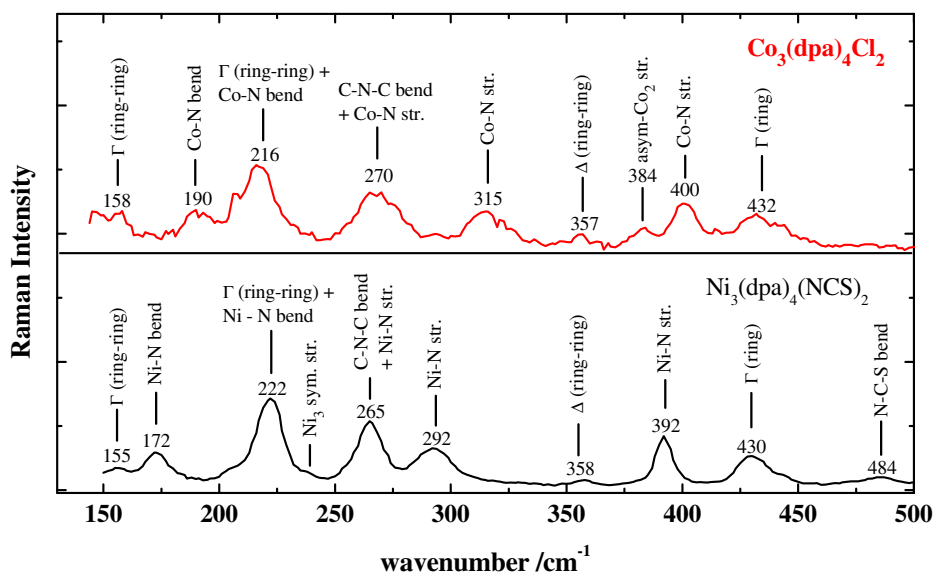
Fig. 5. Raman spectra of $Ni_3(dpa)_4(NCS)_2$ and $Co_3(dpa)_4Cl_2$ in their crystal form mixed with KBr (ratio1:10), excited at 632.8 nm. Symbols are defined in the caption of Fig. 1.

symmetric and asymmetric stretching frequencies of metal trimers to lie in a range 150–350 cm^{-1} depending on the metal–metal bonding [24]; for our metal–metal bond order $\leqslant 1$, the frequencies should fall in this range. Second, for linear trimetals the asymmetric stretching is expected to be strongly active in the infrared and the symmetric stretching mode strongly active in Raman spectra. Moreover, the metal–related line intensity is enhanced in resonance Raman spectra because we excite the molecules in the red-end of their d–d transition. This visible band is assigned by Clerac et al. based on the results of electronic circular dichroism spectroscopy [10]. Third, for a linear geometry the frequency of the asymmetric stretching mode is expected to exceed that of the symmetric mode. Fourth we expect that the frequency shift for the metal–metal stretch is significant when altering from Ni to Co because of a large variation of bond order.

On this basis we assign IR lines at 304 and 311 cm^{-1} to a Ni_3 asymmetric stretching mode, and 282 and 287 cm^{-1} to a Ni-N(dpa) stretching mode for $Ni_3(dpa)_2Cl_2$ and $Ni_3(dpa)_2(NCS)_2$, respectively. The Raman line observed at 242 cm^{-1} is assigned to

the Ni_3 symmetric stretching mode for $Ni_3(dpa)_2Cl_2$ but for $Ni_3(dpa)_2(NCS)_2$ this line appears as a shoulder beside an intense line 222 cm^{-1}. A line for the Co_3 asymmetric stretching mode appears at 313, 331 cm^{-1} and for the Co–N(dpa) stretching mode at 291, 306 cm^{-1} for sym-$Co_3(dpa)_2Cl_2$ and $Co_3(dpa)_2(NCS)_2$, respectively. As the signal for the Co_3 symmetric stretching mode is either too weak or overlapped, we suggest no assignment for this mode. We assign a Raman line at 384 cm^{-1} to the Co–Co stretching mode in an asymmetric structure. The lines below 200 cm^{-1} are attributed to pyridyl–pyridyl, out-of-plane deformation and M–N (dpa) bending modes as indicated in Figs. 3–5. The metal–Cl stretching mode is associated with lines 187 and 201 cm^{-1} for Co_3 and Ni_3 complexes, respectively. The axial-ligand NCS bending mode is assigned at 479 cm^{-1} in IR and 484 cm^{-1} in Raman spectra.

Our data show that the metal–metal binding agrees with a prediction of molecular-orbital theory that the Co–Co binding is nearly a single bond in the asymmetric form. According to these assignments, the Ni–Ni bond is expected to be weak; in addition the frequency assigned to the Ni–Ni stretching mode is for a

normal mode vibrational motion involving also ligands. The contribution to the strength of metal binding from coupling through the central, diamagnetic Ni by two terminal high-spin Ni ions cannot be estimated in the current work. Although the vibrational spectra are complicated, we have been able to identify the metal–metal bonding of these complexes. The sophisticated quantum-chemical calculations are required to obtain accurate geometries and to provide information to definitely assign vibrational spectra.

Acknowledgments

References

[1] S. Aduldecha, B. Hathaway, J. Chem. Soc. Dalton Trans. (1991) 993.
[2] E.C. Yang, M.-C. Cheng, M.S. Tsai, S.M. Peng, J. Chem. Soc. Chem. Commun (1994) 2377.
[3] F.A. Cotton, L.M. Daniels, G.T. Jordan IV, Chem. Commun. (1997) 421.
[4] F.A. Cotton, L.M. Daniels, G.T. Jordan, C.A. Murillo, J. Am. Chem. Soc. 119 (1997) 10377.
[5] R. Clerac, F.A. Cotton, K.R. Dunbar, C.A. Murillo, I. Pascual, X. Wang, Inorg. Chem. 38 (1998) 2655.
[6] F.A. Cotton, C.A. Murillo, X. Wang, J. Chem. Soc. Dalton Trans. (1999) 3327.
[7] F.A. Cotton, C.A. Murillo, X. Wang, Inorg. Chem. 38 (1999) 6294.
[8] R. Clerac, F.A. Cotton, K.R. Dunbar, C.A. Murillo, I. Pascual, X. Wang, Inorg. Chem. 38 (1999) 2655.
[9] R. Clerac et al., J. Am. Chem. Soc. 122 (2000) 6226.
[10] R. Clerac, F.A. Cotton, K.R. Dunbar, T. Lu, C.A. Murillo, X. Wang, Inorg. Chem. 39 (2000) 3065.
[11] R. Clerac, F.A. Cotton, L.M. Daniels, K.R. Dunbar, C.A. Murillo, I. Pascual, Inorg. Chem. 39 (2000) 3414.
[12] R. Clerac, F.A. Cotton, S.P. Jeffery, C.A. Murillo, X. Wang, Inorg. Chem. 40 (2001) 1256.
[13] R. Clerac, F.A. Cotton, L.M. Daniels, K.R. Dunbar, C.A. Murillo, X. Wang, J. Chem. Soc. Dalton Trans. (2001) 386.
[14] J.F. Berry, F.A. Cotton, L.M. Daniels, C.A. Murillo, J. Am. Chem. Soc. 124 (2002) 3212.
[15] J.F. Berry, F.A. Cotton, C.A. Murillo, Dalton Trans. (2003) 3015.
[16] J.F. Berry, F.A. Cotton, L.M. Daniels, C.A. Murillo, X. Wang, Inorg. Chem. 42 (2003) 2418.
[17] J.F. Berry, F.A. Cotton, T. Lu, C.A. Murillo, X. Wang, Inorg. Chem. 42 (2003) 3595.
[18] J.F. Berry, F.A. Cotton, C.A. Murillo, B.K. Roberts, Inorg. Chem. 43 (2004) 2277.
[19] S.-Y. Lin et al., J. Phys. Chem. B 108 (2004) 959.
[20] I.-W.P. Chen et al., Angew. Chem. Int. Ed. 45 (2006) 5814.
[21] P. Kiehl, M.-M. Rohmer, M. Benard, Inorg. Chem. 43 (2004) 3151.
[22] D.A. Pantazis, J.E. McGrady, J. Am. Chem. Soc. 128 (2006) 4128.
[23] M. Frisch et al., GAUSSIAN 03, Revision A. 9, Gaussian Inc., Pittsburgh PA, 2003.
[24] B.N. Papas, H.F. Schaefer III, J. Chem. Phys. 123 (2005) 74321.